nature chemical biology

ARTICLE

PUBLISHED ONLINE: 11 JANUARY 2016 | DOI: 10.1038/NCHEMBIO.1999

Protonation of a glutamate residue modulates the dynamics of the drug transporter EmrE

Anindita Gayen[1,2], Maureen Leninger[1,2] & Nathaniel J Traaseth[1]*

Secondary active transport proteins play a central role in conferring bacterial multidrug resistance. In this work, we investigated the proton-coupled transport mechanism for the *Escherichia coli* drug efflux pump EmrE using NMR spectroscopy. Our results show that the global conformational motions necessary for transport are modulated in an allosteric fashion by the protonation state of a membrane-embedded glutamate residue. These observations directly correlate with the resistance phenotype for wild-type EmrE and the E14D mutant as a function of pH. Furthermore, our results support a model in which the pH gradient across the inner membrane of *E. coli* may be used on a mechanistic level to shift the equilibrium of the transporter in favor of an inward-open resting conformation poised for drug binding.

Secondary active transporters provide a primary defense mechanism in conferring multi-drug resistance (MDR) to bacteria. These integral membrane proteins bind and transport lethal compounds across the lipid bilayer and in the process reduce drug toxicity in the cytoplasm[1]. Antiporters from the small multi-drug-resistance (SMR) family represent an excellent system to study ion-coupled transport because of their small size (~100–120 residues) and importance in antiseptic and antibiotic resistance[2] as well as membrane protein evolution[3]. EmrE is a member of this family that carries out drug efflux as a homodimer by coupling transport with the electrochemical potential across the inner membrane of *E. coli*[4]. The available structural models of EmrE depict an antiparallel dimer arrangement[5–7] that stems from the dual-topology insertion in the membrane[3]. Although it is known that a conserved glutamate residue (Glu14) within the first transmembrane (TM) domain of EmrE plays a central role in transport[8], the mechanistic details of how this anionic residue couples efflux with the pH gradient have not been elucidated. In this work, we used a combination of drug-resistance assays and biophysical experiments, including solution and solid-state NMR spectroscopy, to probe the conformational dynamics and allosteric communication within EmrE that underlie the ion-coupled mechanism.

RESULTS

pH titration of EmrE using solution NMR spectroscopy

Since previous work implicated Glu14 as having a direct role in drug efflux[8], we used solution NMR spectroscopy to measure the proton affinity with site-specific resolution. EmrE was isotopically enriched with ^{13}C at all isoleucine $C^{\delta1}$ methyl groups and reconstituted into DMPC/DHPC isotropic bicelles as described previously[9]. The chemical shifts were recorded using $^{1}H/^{13}C$ heteronuclear correlation experiments and were assigned through a single-site mutagenesis method involving the replacement of isoleucine residues with either leucine or valine (example spectra are shown in **Supplementary Results**, **Supplementary Fig. 1**). Similar to our previous observations for drug-free EmrE[9,10], we detected systematic peak doubling for 14 of the 15 isoleucine residues, which stems from the asymmetric nature of the dimer structure[6,7,11] (**Fig. 1a**). The only exception was Ile38, which likely had similar environments for both monomer subunits. Importantly, a spectral comparison of EmrE in DMPC and *E. coli* bicelles showed a remarkable similarity for both the drug-free and drug-bound forms (**Supplementary Fig. 2**), which supports the presence of a native fold under our experimental conditions.

To gauge the effect of acid-base chemistry on the transporter, we varied the pH from 5.0 to 9.15, recording $^{1}H/^{13}C$ SOFAST HMQC[12] correlation spectra at each value. In this titration, several significant chemical shift perturbations near and far from Glu14 were detected, suggesting that the acid-base chemistry had a pronounced effect on the structure of the transporter (**Fig. 1a**). As the pH could affect residues other than Glu14, we carried out a control experiment using the E14Q mutant of EmrE, which was expected to behave like a fully protonated transporter at position 14. No significant perturbations were observed in the titration (**Supplementary Fig. 3a**), confirming that the spectral changes seen for wild-type EmrE resulted from Glu14 protonation and deprotonation. In addition, the E14Q spectrum was much more similar to that of the wild-type protein at low pH than at high pH, which further showed that this mutant is a good mimic of the fully protonated transporter (**Supplementary Fig. 3b**).

To quantify the pH-induced perturbations, the chemical shifts for wild-type EmrE were plotted against the pH. Most residues showed a classical two-state transition, and thus the apparent acid dissociation constant for Glu14 was obtained by fitting 18 ^{1}H and ^{13}C chemical shifts in a global fashion to a modified Henderson-Hasselbalch equation given in equation (1) of the Online Methods (average of the normalized shifts are shown in **Fig. 1b**). The apparent pK_a value of 7.0 ± 0.2 for the wild-type protein at 25 °C was in agreement with the estimated values reported from fluorescence measurements[13]. In addition, individual residues were fit to a single apparent pK_a value, with nearly all residues within the range of 6.8–7.2. It is important to note that our data cannot definitively rule out the possibility of two pK_a values for Glu14. However, we emphasize that the single transition we report reflects the largest chemical shift changes observed in the titration (i.e., most significant structural change) and suggests that the two Glu14 residues in the binding pocket may have the same or similar pK_a values within the experimental error of our measurements. This is also supported by individual fits for each monomer of EmrE, which resulted in apparent pK_a values within 0.1 units of each other (**Supplementary Fig. 4**). To further elucidate the mechanism of the native Glu14 residue in EmrE, we carried out a similar pH titration with an E14D mutant that was previously shown to uncouple drug transport and confer limited drug resistance to *E. coli*[13]. Similar to what was found for E14Q, the aspartate side chain of the mutant showed no major chemical shift changes over the pH range of 6.5–7.5, indicating

[1]Department of Chemistry, New York University, New York, New York, USA. [2]These authors contributed equally to this work. *e-mail: traaseth@nyu.edu

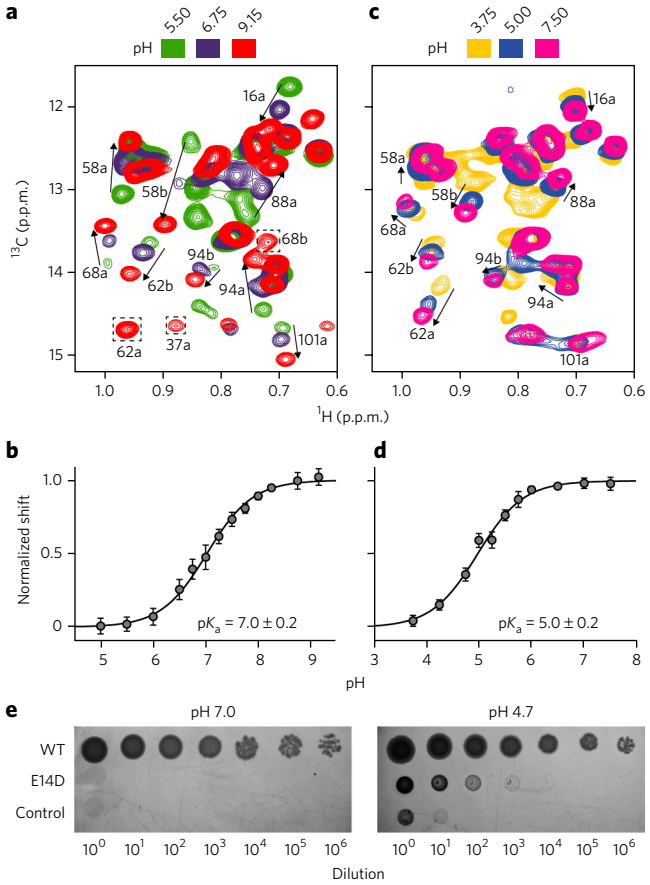

Figure 1 | pH-induced conformational changes to EmrE. (**a**–**d**) Overlay of ^{1}H/^{13}C SOFAST-HMQC NMR spectra for isoleucine methyl groups at the indicated pH values for (**a**) wild-type (WT) and (**c**) E14D EmrE; dotted boxes indicate peaks that disappeared as the pH was dropped to more acidic values. Arrows indicate the direction of chemical shift changes from low to high pH. (**b**,**d**) Normalized chemical shift perturbations at 25 °C for wild-type and E14D EmrE, respectively. The global fit to individual sites gave the indicated apparent pK_a values of 7.0 and 5.0. The error bars reflect the standard deviation among residues used to construct the fit. (**e**) *E. coli* resistance assays using serial ten-fold dilutions in the presence of an LB agar plate with 240 μM ethidium bromide and carbenicillin. The assays were performed at pH 7.0 and 4.7 using wild-type EmrE, E14D and a control that contained no expressed EmrE. Control dilution experiments in the absence of ethidium are shown in **Supplementary Figure 13**. The resistance assay was repeated with similar results at least five times.

an altered pK_a for Asp14 (**Supplementary Fig. 3a**). Upon further reduction of pH, we observed spectral perturbations similar to those observed for the wild type that enabled us to determine the more acidic apparent pK_a value of 5.0 ± 0.2 (**Fig. 1c**,**d**).

Ethidium resistance assays of EmrE and the E14D mutant

With the apparent acid dissociation constant of the conserved anionic residue determined, we aimed to understand how the acidity might affect the resistance phenotype for E14D and wild-type EmrE as a function of pH. Ethidium bromide resistance assays were carried out with *E. coli* transformed with plasmids encoding wild-type and E14D EmrE at pH 7.0 and pH 4.7 using a ten-fold serial dilution assay to assess the phenotype conferred by the transporter. The results at neutral pH showed that only wild-type EmrE conferred resistance relative to control vector (**Fig. 1e**; growth up to 10^6 dilution) and are in agreement with previous findings that showed E14D to be essentially inactive under these conditions[14]. To the contrary, the resistance assays carried out at pH 4.7 indicated that E14D was able to confer a detectable phenotype at a dilution factor of up to 10^4, whereas the control grew only at a ten-fold dilution (**Fig. 1e**). Because this phenotype was not observed at pH 7.0, these results support the conclusion that the pK_a should be approximately between the pH values of the cytoplasm (~7.6) and periplasm (same as the external environment[15]) in order to confer catalytic competency for coupling drug efflux with proton transport. This conclusion is consistent with the competition model proposed for EmrE[4].

pH-dependent conformational dynamics of EmrE

The alternating access model requires a transporter to exchange between at least two major conformations to carry out transport of drugs and protons (that is, inward-open and outward-open; see model in **Fig. 2a**)[16]. Because of the associated angular changes of the helices within the membrane, the oriented solid-state NMR approach is a sensitive method to capture these conformational changes in a direct fashion[17,18]. We previously showed that each monomer within the EmrE dimer possesses different helical tilt angles with respect to the bilayer surface[10], with the two peaks for each residue in the oriented NMR spectrum corresponding to the monomers within the asymmetric dimer[5,7]. Because these two populations interconvert on the millisecond-to-second timescale[9] and the conformational dynamics of EmrE are necessary for ethidium efflux across membranes[19], these previous findings establish the ability to monitor exchange dynamics between inward-open and outward-open conformations using NMR spectroscopy in bicelles. To directly probe the exchange dynamics of EmrE as a function of pH, we used the PUREX method[20] in magnetically aligned lipid bicelles (DMPC/DHPC, 3.5:1), which has been previously implemented in our laboratory[9]. Similar to the pH titration experiments, we recorded a series of PUREX data sets over a range of pH values (**Supplementary Fig. 5**). The quantified exchange rates showed that the fastest conversion between inward-open and outward-open states occurred at acidic pH values, whereas slower rates were observed at pH values above the apparent pK_a for Glu14 (**Fig. 2b**,**c**). In support of these measurements, methyl T_{1zz} NMR experiments were recorded at pH 9.15 (~2 units above the apparent pK_a) using solution NMR and also showed intense exchange peaks between the two populations that were consistent with the PUREX results (**Fig. 2d**). These data suggest an apparent two-state dynamic exchange process in which the conformational flipping rates are equal to 220 s^{-1} and 40 s^{-1} for the fully protonated (pH 5.8) and deprotonated (pH 8.4) transporter, respectively. Although the rates were obtained in the absence of the membrane potential and could be further influenced within the cell membrane of the organism, the reduced exchange rate of the deprotonated state is in qualitative agreement with the coupling rules proposed for ion-coupled antiport[21].

Validation of conformational equilibrium in ΔpH liposomes

Based on the difference in rate constants between the protonated and deprotonated states of EmrE, we predicted that the presence of a pH gradient (ΔpH) across a lipid bilayer and centered around the pK_a of Glu14 would bias EmrE's open conformation toward the higher-pH side of the membrane. To test this hypothesis, we designed a tryptophan fluorescence assay in liposomes encompassing a ΔpH across the bilayer. Because the fluorescence emission profile of tryptophan is sensitive to the protonation state of Glu14 (deprotonated Glu14 results in high fluorescence, protonated in low fluorescence)[13], the spectrum was used to determine the preferred orientation of inward- or outward-facing EmrE. Spectra were recorded for wild-type EmrE in four samples possessing the following pH^{in}/pH^{out} combinations: (i) 8.7/6.2, (ii) 6.2/8.7, (iii) 6.2/6.2 and (iv) 8.7/8.7. The fluorescence signatures for the ΔpH vesicles are shown in **Figure 2e** and were found to be intermediate with respect to control vesicles that had the same pH on both sides of the membrane. Because protonation and

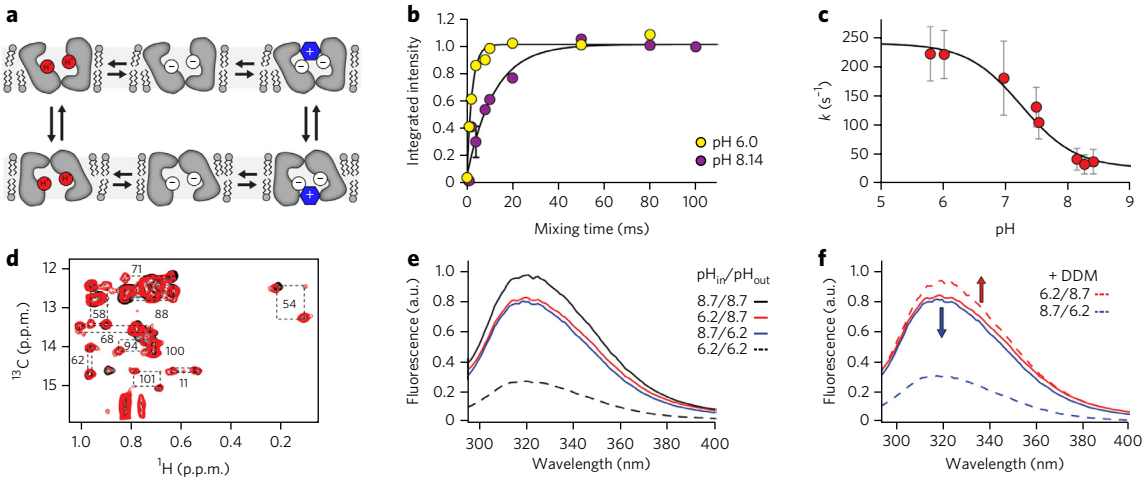

Figure 2 | Glu14 protonation sets the resting state. (**a**) Schematic of the alternating access model. The vectorial transport rules forbid conformational exchange in the fully unloaded transporter[21]. (**b**) Conformational exchange dynamics probed with PUREX in aligned bicelles at the two indicated pH values. (**c**) Quantified exchange rates as a function of pH (error bars reflect a 90% confidence interval). All of the PUREX curves used to construct panel **c** are shown in **Supplementary Figure 5**. (**d**) Overlay of a methyl T_{1zz} experiment (red) and HSQC spectrum (black) of deprotonated EmrE (pH 9.15). The dotted boxes connect the two exchanging peaks and support the presence of conformational dynamics in the deprotonated Glu14 transporter. A control T_{1zz} experiment carried out with cross-linked EmrE showed no exchange peaks, supporting the conclusion that the exchange peaks for wild-type EmrE reflect a conformational change consistent with the alternating access model (**Supplementary Fig. 14**). (**e**) Tryptophan fluorescence of EmrE in DMPC vesicles under different pH combinations. (**f**) Disruption of the ΔpH vesicles through addition of DDM detergent. The same fluorescence result was obtained in three independent trials.

deprotonation are expected to occur faster than the conformational change[13], the relative signal intensities were used to estimate that ~83% of EmrE dimers were oriented in an open conformation toward the basic pH side of the bilayer, in agreement with the rates measured from NMR. Note that disrupting the pH gradient caused the fluorescence spectra to look similar to those of the respective high- and low-pH controls, which confirmed the conformational preference in the asymmetric vesicles (**Fig. 2f**). Similar results were also obtained in *E. coli* lipid vesicles (**Supplementary Fig. 6**) and therefore support the conclusion that a pH gradient can influence the conformational equilibrium of a transporter in a native-like lipid composition.

Long-range allosteric communication

Why does protonation of Glu-14 affect the exchange kinetics? To delve into the mechanism, we mapped the isoleucine chemical shift perturbations between the protonated and deprotonated forms of Glu14 onto the X-ray structure of EmrE bound to tetraphenylphosphonium (TPP^+)[7]. Note that owing to the resolution of the structure (3.8 Å, C_α model), the isoleucine methyl group chemical shift changes were plotted at the α-carbon positions. Perturbations were observed in all TM domains of the transporter, including loop 2 connecting TM-2 with TM-3, as well as significant changes within TM-4, which is involved in dimer stability (**Fig. 3a**)[7,22,23]. These changes persisted up to ~25 Å from the substrate-binding pocket containing Glu14 and were indicative of a long-range allosteric effect. Interestingly, chemical shift perturbation mapping for E14D showed dramatically attenuated changes for the mutant as compared with the wild-type protein (**Fig. 3b**), which suggested that the shorter side chain partially disrupted the allosteric communication within the transporter. A surprising finding for wild-type EmrE was that the perturbations to loop 2

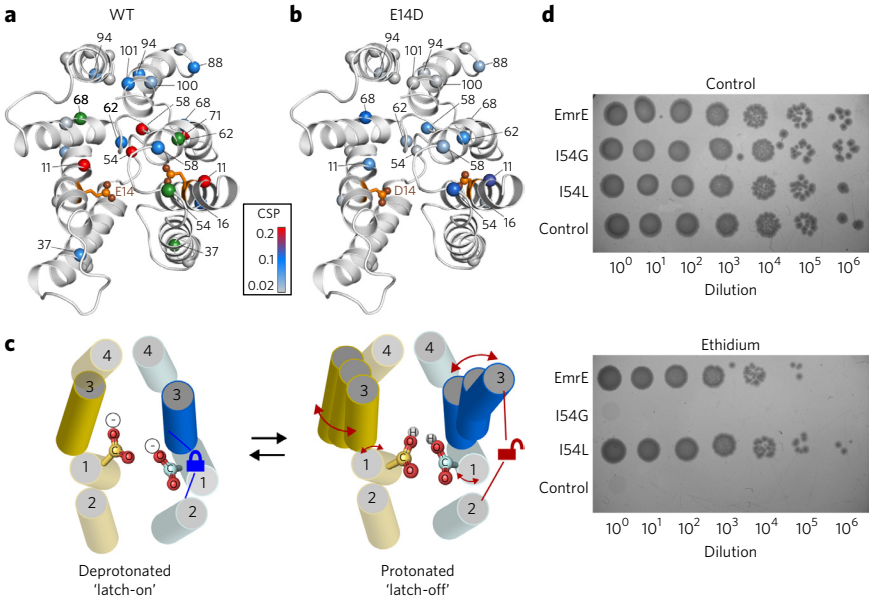

Figure 3 | Allosteric conformational change from Glu14 protonation. (**a**) Heat map of the chemical shift perturbations (CSP) between pH 5.5 and pH 9.15 mapped onto the Cα atoms of EmrE (PDB 3B5D)[7]. Green spheres denote residues whose signals became too weak to be followed in the pH titration below ~7.0. (**b**) Perturbation data for E14D EmrE mapped onto the same structure (difference between pH 3.75 and pH 7.5). Both perturbation data sets are viewed from the perspective of the open side of the transporter. (**c**) Cartoon model illustrating the proposed role of the latch in stabilizing the open conformation of EmrE, which is consistent with the NMR perturbations in the pH titration, the analysis of the crystal structure of EmrE and the loss of resistance for I54G. The TM domains are indicated with numbers. (**d**) *E. coli* resistance assays carried out using serial ten-fold dilutions on an LB agar plate (pH 7) containing carbenicillin in the absence (top) and presence (bottom) of 240 μM ethidium bromide. The plasmid contained wild-type, I54G or I54L EmrE or was a control vector in which EmrE was not expressed. The resistance assay was repeated twice with the same result.

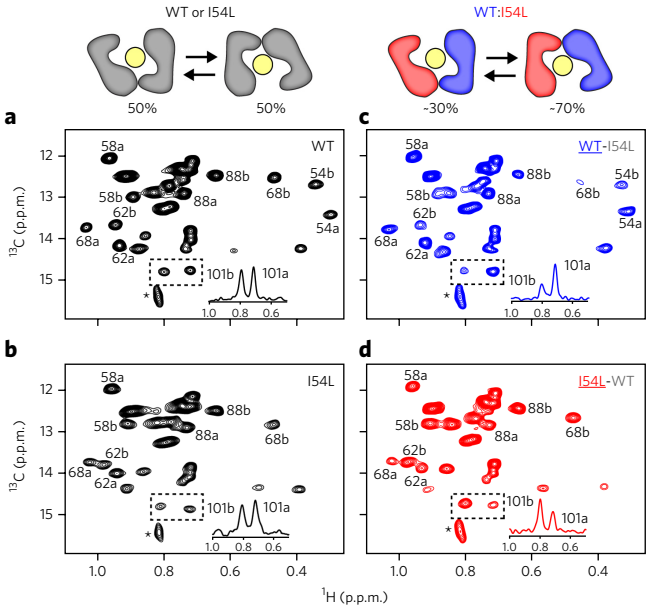

Figure 4 | Conformational bias from loop 2 mutant in mixed EmrE dimers. (**a**,**b**) ^{1}H/^{13}C SOFAST-HMQC experiments with wild-type (**a**) and I54L (**b**) EmrE in the presence of TPP^{+}. (**c**,**d**) Two similar experiments with mixed dimers of wild-type and I54L EmrE in which one or the other protein (indicated by underlining) was ^{13}C enriched. The mixed sample in which I54L was NMR enriched gave more intense peaks for monomer "b," whereas the labeled wild type gave greater peak intensities for monomer "a." Insets within the HMQC spectra show one-dimensional slices for Ile101 to illustrate the skewed populations. The dotted box shows the two peaks for Ile101. The asterisks indicate lipid peaks.

adjoining TM2 and TM3 were different on one side of the transporter than on the other. For example, the peaks corresponding to Ile54 and Ile62 within the inward-open face became very weak and disappeared upon protonation of Glu14, whereas these same residues on the other monomer showed large chemical shift changes without significant intensity reductions (**Supplementary Fig. 7**). These asymmetric perturbations, combined with analysis of the EmrE crystal structure, support a 'latching model' of loop 2 to stabilize the open configuration of the transporter by excluding the N-terminal side of TM1 from the substrate-binding chamber (**Fig. 3c** and **Supplementary Fig. 8**). We propose that Glu14 protonation leads to the disruption of these contacts, resulting in large chemical shift perturbations and the observed conformational broadening of loop 2.

To further investigate the mechanistic features of loop 2, we engineered mutants at residue 54 (I54G and I54L) and performed resistance assays in *E. coli*. Interestingly, the I54G substitution completely abolished the resistance to ethidium, but the I54L mutation produced no loss of function beyond that of wild-type EmrE (**Fig. 3d**). The former is consistent with literature reports that I54C EmrE was a partial loss-of-function mutant[23,24]. Taken together with homology modeling showing the conservation of residue 54 as a large and hydrophobic amino acid residue (isoleucine, leucine, valine or methionine)[25], these findings implicate Ile54 as an important site in loop 2.

EmrE heterodimers to probe asymmetry of loop 2

In the process of assigning Ile54 in the methyl HMQC spectrum, we serendipitously discovered that I54L did not show peak doubling such as was observed for wild-type EmrE (**Supplementary Fig. 9**). Although this mutant did not disrupt the ability to confer drug resistance (**Fig. 3d**), we surmised that it might be useful for providing insight into the asymmetry of loop 2. As anticipated from the resistance assay, I54L was able to bind drugs and upon addition of TPP^{+} gave two populations similar to those for wild-type EmrE (**Fig. 4a**,**b**). These results imply that the conformational exchange for I54L in the absence of drug was greater than that for the wild-type protein. On the basis of these findings and the asymmetric behavior of Ile54 in the wild-type pH titration, we predicted that a heterodimer mixing experiment might break the 50/50 population of the NMR resonances. We also anticipated that this experiment would give insight into which of the two I54L mutations in the asymmetric dimer had a more pronounced effect on the dynamics. The experiment was carried out by preparing a 2:1 sample of I54L (without ^{13}C incorporation) and wild-type EmrE ($^{13}C_{\delta}$-isoleucine methyl labeled) and recording the ^{1}H/^{13}C isoleucine methyl spectrum. Remarkably, we observed ~2-fold more intense signals from one set of monomer peaks than from the other in both DMPC (**Fig. 4c**) and *E. coli* bicelles (**Supplementary Fig. 10**). The opposite isotopic labeling experiment, in which I54L EmrE was enriched and wild-type EmrE was unlabeled, gave more intense signals for the other set of monomer resonances (**Fig. 4d**). To further substantiate the results for Ile54, we also carried out a second mixed-dimer experiment with I62L—the other residue in loop 2 that displayed heterogeneity during the pH titration. Consistent with our results for I54L, the mixed dimer of isotopically enriched I62L and unlabeled wild type also showed a conformational bias toward the same set of monomer resonances as for I54L (**Supplementary Fig. 11**). Therefore, the ability to influence the ratio of the two populations underscores the fact that the asymmetric contacts stabilize the EmrE structure. Furthermore, although I54L did not disrupt the phenotype, indicating that it was unable to influence the rate-limiting step in the transport cycle, these results support a differential stabilizing role for loop 2 between the open and closed sides of the transporter. Taken together with our previous results showing a well-defined structure for the loop adjoining TM3 and TM4 (ref. 26), these findings strongly imply an active role for loops in the allosteric communication network and ion-coupled transport process.

DISCUSSION

The findings described in this article unveil mechanistic details governing active transport in the SMR family modulated by acid-base chemistry of a conserved anionic residue. At pH values above the apparent pK_a of Glu14, our dynamics measurements indicated significantly reduced conformational exchange relative to the protonated form, which is consistent with vectorial transport rules[21]. However, in contrast to these strict rules that encompass perfect coupling of pH gradients with drug efflux, we observed small but significant conformational dynamics in the proton-unloaded form, suggesting that a minor population of EmrE might possess an outward-open conformation facing the periplasm under equilibrium conditions. A couple of key observations in cases where the pH gradient is solely responsible for transport (i.e., divalent cations[27]) suggest that nonzero exchange under our experimental conditions may have significance *in vivo*. The first is the observation of polyamine import in the W63G mutant of EmrE, which implies the presence of an outward-open facing conformation[28]. This finding also suggests that Trp63 may play an important role in transmitting the allosteric communication and conformational changes we observed upon protonation at Glu14. A second relevant finding is that EmrE sensitizes *E. coli* to methyl viologen under alkaline growth conditions where $pH_{periplasm} > pH_{cytoplasm}$[27]. Relevant to this, we carried out resistance assays on E14D and wild-type EmrE and found that the mutant conferred sensitivity to methyl viologen at pH 7.0 (**Supplementary Fig. 12**). The latter two observations of drug sensitivity support net drug import into the cytoplasm and imply an outward-facing conformation that is consistent with predictions from the NMR dynamics measurements. Interestingly, drug import has also been observed in single-site mutants of SugE[29], which is a protein closely related to EmrE and a member of the SMR family. Future studies

will need to investigate the conformational dynamics under native growth conditions to determine the role of the membrane potential as well as to further probe the allosteric communication network responsible for conformational switching in the membrane.

Received 29 January 2015; accepted 10 November 2015; published online 11 January 2016

METHODS

Methods and any associated references are available in the online version of the paper.

References

1. Higgins, C.F. Multiple molecular mechanisms for multidrug resistance transporters. *Nature* **446**, 749–757 (2007).
2. Bay, D.C., Rommens, K.L. & Turner, R.J. Small multidrug resistance proteins: a multidrug transporter family that continues to grow. *Biochim. Biophys. Acta* **1778**, 1814–1838 (2008).
3. Rapp, M., Seppälä, S., Granseth, E. & von Heijne, G. Emulating membrane protein evolution by rational design. *Science* **315**, 1282–1284 (2007).
4. Schuldiner, S. in *Membrane Transport Mechanism* (ed. Krämer, R.Z. & Ziegler, C.) 233–248 (Springer, Berlin, 2014).
5. Fleishman, S.J. *et al.* Quasi-symmetry in the cryo-EM structure of EmrE provides the key to modeling its transmembrane domain. *J. Mol. Biol.* **364**, 54–67 (2006).
6. Ubarretxena-Belandia, I., Baldwin, J.M., Schuldiner, S. & Tate, C.G. Three-dimensional structure of the bacterial multidrug transporter EmrE shows it is an asymmetric homodimer. *EMBO J.* **22**, 6175–6181 (2003).
7. Chen, Y.J. *et al.* X-ray structure of EmrE supports dual topology model. *Proc. Natl. Acad. Sci. USA* **104**, 18999–19004 (2007).
8. Muth, T.R. & Schuldiner, S. A membrane-embedded glutamate is required for ligand binding to the multidrug transporter EmrE. *EMBO J.* **19**, 234–240 (2000).
9. Cho, M.K., Gayen, A., Banigan, J.R., Leninger, M. & Traaseth, N.J. Intrinsic conformational plasticity of native EmrE provides a pathway for multidrug resistance. *J. Am. Chem. Soc.* **136**, 8072–8080 (2014).
10. Gayen, A., Banigan, J.R. & Traaseth, N.J. Ligand-induced conformational changes of the multidrug resistance transporter EmrE probed by oriented solid-state NMR spectroscopy. *Angew. Chem. Int. Edn Engl.* **52**, 10321–10324 (2013).
11. Morrison, E.A. *et al.* Antiparallel EmrE exports drugs by exchanging between asymmetric structures. *Nature* **481**, 45–50 (2012).
12. Schanda, P. & Brutscher, B. Very fast two-dimensional NMR spectroscopy for real-time investigation of dynamic events in proteins on the time scale of seconds. *J. Am. Chem. Soc.* **127**, 8014–8015 (2005).
13. Adam, Y., Tayer, N., Rotem, D., Schreiber, G. & Schuldiner, S. The fast release of sticky protons: kinetics of substrate binding and proton release in a multidrug transporter. *Proc. Natl. Acad. Sci. USA* **104**, 17989–17994 (2007).
14. Yerushalmi, H. & Schuldiner, S. An essential glutamyl residue in EmrE, a multidrug antiporter from *Escherichia coli*. *J. Biol. Chem.* **275**, 5264–5269 (2000).
15. Wilks, J.C. & Slonczewski, J.L. pH of the cytoplasm and periplasm of *Escherichia coli*: rapid measurement by green fluorescent protein fluorimetry. *J. Bacteriol.* **189**, 5601–5607 (2007).
16. Jardetzky, O. Simple allosteric model for membrane pumps. *Nature* **211**, 969–970 (1966).
17. Wang, J. *et al.* Imaging membrane protein helical wheels. *J. Magn. Reson.* **144**, 162–167 (2000).
18. Marassi, F.M. & Opella, S.J. A solid-state NMR index of helical membrane protein structure and topology. *J. Magn. Reson.* **144**, 150–155 (2000).
19. Dutta, S., Morrison, E.A. & Henzler-Wildman, K.A. Blocking dynamics of the SMR transporter EmrE impairs efflux activity. *Biophys. J.* **107**, 613–620 (2014).
20. deAzevedo, E.R., Bonagamba, T.J. & Schmidt-Rohr, K. Pure-exchange solid-state NMR. *J. Magn. Reson.* **142**, 86–96 (2000).
21. Jencks, W.P. Utilization of binding energy and coupling rules for active transport and other coupled vectorial processes. *Methods Enzymol.* **171**, 145–164 (1989).
22. Poulsen, B.E., Rath, A. & Deber, C.M. The assembly motif of a bacterial small multidrug resistance protein. *J. Biol. Chem.* **284**, 9870–9875 (2009).
23. Amadi, S.T., Koteiche, H.A., Mishra, S. & McHaourab, H.S. Structure, dynamics, and substrate-induced conformational changes of the multidrug transporter EmrE in liposomes. *J. Biol. Chem.* **285**, 26710–26718 (2010).
24. Mordoch, S.S., Granot, D., Lebendiker, M. & Schuldiner, S. Scanning cysteine accessibility of EmrE, an H^+-coupled multidrug transporter from *Escherichia coli*, reveals a hydrophobic pathway for solutes. *J. Biol. Chem.* **274**, 19480–19486 (1999).
25. Brill, S., Sade-Falk, O., Elbaz-Alon, Y. & Schuldiner, S. Specificity determinants in small multidrug transporters. *J. Mol. Biol.* **427**, 468–477 (2015).
26. Banigan, J.R., Gayen, A., Cho, M.K. & Traaseth, N.J. A structured loop modulates coupling between the substrate-binding and dimerization domains in the multidrug resistance transporter EmrE. *J. Biol. Chem.* **290**, 805–814 (2015).
27. Rotem, D. & Schuldiner, S. EmrE, a multidrug transporter from *Escherichia coli*, transports monovalent and divalent substrates with the same stoichiometry. *J. Biol. Chem.* **279**, 48787–48793 (2004).
28. Brill, S., Falk, O.S. & Schuldiner, S. Transforming a drug/H^+ antiporter into a polyamine importer by a single mutation. *Proc. Natl. Acad. Sci. USA* **109**, 16894–16899 (2012).
29. Son, M.S. *et al.* Mutagenesis of SugE, a small multidrug resistance protein. *Biochem. Biophys. Res. Commun.* **312**, 914–921 (2003).

Acknowledgments

This work was supported by US National Institutes of Health (NIH) grant R01AI108889 and start-up funds from New York University (NYU) to N.J.T. M.L. acknowledges support from a Margaret Strauss Kramer Fellowship. The NMR data collected with a cryoprobe at NYU was supported by an NIH S10 grant (OD016343). Data collected at the New York Structural Biology Center was made possible by a grant from NYSTAR. The authors thank R. Turner at the University of Calgary for providing wild-type EmrE in the pMS119EH vector, M.-K. Cho for assistance of the initial NMR experiments, A. Sae Her for assistance in protein purification, and D. Buccella at NYU for use of the spectrofluorometer.

Author contributions

N.J.T. designed the project. A.G. and M.L. carried out the solution NMR, solid-state NMR, fluorescence experiments and ethidium resistance assays. All authors analyzed the data. N.J.T. wrote the manuscript.

Competing financial interests

The authors declare no competing financial interests.

Additional information

Any supplementary information, chemical compound information and source data are available in the online version of the paper. Reprints and permissions information is available at www.nature.com/reprints/index.html. Correspondence and requests for materials should be addressed to N.J.T. (traaseth@nyu.edu).

ONLINE METHODS

Protein expression and purification. The expression and purification of EmrE was carried out as previously described[10]. Briefly, EmrE was expressed as a fusion construct with maltose-binding protein and purified using affinity and size exclusion chromatography in *n*-dodecyl-β-D-maltopyranoside (DDM, Anatrace). [Ile-$^{13}CH_3$, U-^{15}N, ^{2}H]-labeled EmrE was expressed with addition of 50 mg/L 2-ketobutyric acid-4-^{13}C, 3,3-$^{2}H_2$ sodium salt hydrate 1 h before induction. The wild-type and E14D pH titrations to measure the acid dissociation constants (pK_a) utilized ^{2}H background labeling and protonation at the Ile methyl groups. Isotopic enrichment for oriented solid-state NMR was accomplished by growing bacteria in the presence of ^{15}N NH_4Cl.

NMR sample preparation. For solution NMR studies, EmrE in DDM was reconstituted in 10% (w/v) dimyristoyl-*sn*-glycero-3-phosphocholine/dihexanoyl-*sn*-glycero-3-phosphocholine (DMPC/DHPC) bicelles (q = 0.33) with the lipid chains having perdeuteration (14:0 PC D54 and 6:0 PC D22, Avanti Polar Lipids). *E. coli* isotropic bicelles were prepared in a similar fashion by replacing DMPC with *E. coli* polar lipid extract from Avanti Polar Lipids. Ile methyl resonance assignments were obtained with single-site mutants prepared with the single-site mutagenesis kit from Agilent (Ile to either Val or Leu). The final NMR samples for solution NMR contained 0.5 mM EmrE, 20 mM Na_2HPO_4, 20 mM NaCl, 50 mM DTT and 0.02% NaN_3.

Solution NMR spectroscopy. Solution NMR experiments were performed with NMR spectrometers operating at a ^{1}H frequency of 600 MHz. For the pH titrations, $^{1}H/^{13}C$ SOFAST-HMQC experiments[12] were acquired at 15 °C and 25 °C using a spectral width for ^{1}H and ^{13}C was 12,019.2 Hz (83.2 ms acquisition time) and 4,000 Hz (27.5 ms evolution time), respectively and a recycle delay of 1 s. The pH was monitored before and after each HMQC experiment and was found to fluctuate by only ±0.01.The complete pH titration curve was collected over ~1–2 days and residues showing significant chemical shift perturbations (^{1}H > 0.03 p.p.m. and ^{13}C > 0.1 p.p.m.) were globally fit using equation (1), where δ_{HA} and δ_{A-} are the chemical shifts for the protonated and deprotonated transporter, respectively, while δ is the observed chemical shift at the different pH values.

$$\delta = \frac{\delta_{HA} + \delta_{A-}10^{pH-pKa}}{1+10^{pH-pKa}} \quad (1)$$

The combined chemical shift perturbation between protonated and deprotonated EmrE at Glu14 ($\Delta\delta$) in the ^{13}C ($\Delta\delta_C$) and ^{1}H ($\Delta\delta_H$) dimensions of the methyl spectra was calculated using a ^{13}C scaling factor of 0.184 with the equation below.

$$\Delta\delta = \sqrt{(0.184\Delta\delta_C)^2 + \Delta\delta_H^2} \quad (2)$$

Methyl T_{1zz} exchange spectra were acquired with a mixing time 300 ms and a recycle delay of 1 s.

Solid-state NMR spectroscopy. Oriented solid-state NMR experiments were carried out using [U-^{15}N] EmrE at a concentration of ~2 mM in 25% DMPC/DHPC (w/v) bicelles at 37 °C. The HEPES concentration was increased to 150 mM to maintain pH control during the experiment. $YbCl_3$ was added to a final concentration of 3 mM to induce alignment of the bilayer normal parallel with respect to the magnetic field. For all experiments, the pH was checked before and after the experiments and found to be within ±0.05 units. The PUREX experiment[20] was acquired on an Agilent DD2 spectrometer operating at a ^{1}H frequency of 600 MHz. A tau value of 0.25 ms was used for both the modulated and reference data sets. The range of mixing times was varied from 0.125 to 800 ms depending on the sample exchange rate. Acquisition of select mixing times in duplicate experiments were used to estimate the error. The modulated and reference spectra were acquired with 2,048 scans and 512 scans, respectively, which was needed to normalize the signal to noise ratio. The PUREX curve for each pH point required ~4–6 days of experimental acquisition time. The two data sets were subtracted to obtain the difference spectrum, which gave only signal intensities due to the exchange cross-peaks. The integrated spectra were plotted with respect to their mixing time and fit to the following equation to calculate the exchange rate (k_{ex}):

$$I_{AB}(t) = k_1(1 - e^{-k_{ex}t}) + k_3 \quad (3)$$

k_1 and k_3 are scaling factors to compensate for the signal intensities between different samples and a y-axis offset, respectively. The data were fit to obtain k_{ex} with the rate constants reported as k values in the text (i.e., $k = k_{ex}/2$). The errors reported in these values reflect the fitted error at a 90% confidence interval. All ^{15}N spectra were referenced to 41.5 p.p.m. with the use of $^{15}NH_4Cl$(s).

Preparation of ΔpH vesicles. Reconstitutions into the asymmetric pH membranes was accomplished through *n*-decyl-β-D-maltoside (DM, Anatrace) detergent by reconstituting the protein at a given pH and pelleting of the vesicles by ultracentrifugation followed by a gentle resuspension to the desired pH on the external side of the liposomes. Wild-type EmrE was reconstituted in DMPC or *E. coli* polar lipid extract (Avanti Polar Lipids, Inc.) where the pH values inside/outside the vesicles were set as pH^{in}/pH^{out}: 6.2/6.2, 6.2/8.7, 8.7/6.2, and 8.7/8.7. The buffer condition was 50 mM sodium phosphate and 20 mM NaCl. After reconstitution the proteoliposomes were centrifuged for 1.5 h at 130,000*g* and resuspended in the same buffer as that in the interior of the vesicles. This cycle was done a total of two times to ensure control of the inside pH. Prior to collection of the fluorescence spectra, the proteoliposomes were diluted 30-fold with the external buffer. After collection of the ΔpH experiments, a small amount of stock DDM was added (final ratio of DDM/lipid = 1/50, mol/mol) to disturb the pH gradient. Since the volume outside the vesicles was greater than that inside, the pH of the interior changed to the external value.

Fluorescence measurements in ΔpH vesicles. EmrE in 5 mM DM detergent was reconstituted to a final concentration of 0.5 μM into 175 μM lipids (either DMPC or *E. coli* lipid extract). Steady-state fluorescence experiments were carried out with an excitation wavelength (λ_{ex}) of 280 nm and an emission wavelength (λ_{em}) range of 200–400 nm with excitation and emission bandwidths of 2 nm and 4 nm, respectively. The emission range was chosen to confirm that Rayleigh scattering for all the ΔpH vesicles were similar. All the vesicles were incubated for 5 min at 25 °C before data collection. The data was an average of 2 scans. Each individual experiment was repeated two or more times. The uncorrected fluorescence data were directly plotted against all samples carried out in the same data set. To make the plots, the relative fluorescence value on the y-axis was normalized to 1.0; no other normalization was performed on the data.

Resistance assays. The PMS119EH vector for the ethidium bromide resistance assay was a gift from R. Turner (University of Calgary). The cells containing vector were grown at 37 °C in an LB medium up to an OD_{600} = 1.0. The bacteria were spotted onto carbenicillin-supplemented LB agar plates at a range of dilutions (10^0 to 10^6). LB media for the plates and ethidium bromide stock solutions were buffered with 10 mM MOPS. The vector with no ribosome-binding site for the *EmrE* gene was selected as a control for the assay. The ethidium bromide concentration was 240 μM.

doi:10.1038/nchembio.1999